

Exclusive vector meson production at HERMES

Aram Movsisyan^a on behalf of the HERMES Collaboration

INFN-University of Ferrara, via Saragat 1, 44122 Ferrara, Italy

Abstract. Exclusive electroproduction of vector mesons has been measured on hydrogen and deuterium targets at HERMES using the 27.6 GeV electron/positron beam of HERA. From this process, more information can be obtained about generalized parton distributions (GPDs), which provide a unified description of the structure of hadrons embedding longitudinal-momentum distributions (ordinary PDFs) and transverse-position information (form factors). The study of the azimuthal distribution of the decay products via spin-density matrix elements provide constraints on helicity-amplitudes used to describe exclusive vector-meson production. Recent results from the HERMES experiment on the production of rho, omega and phi mesons will be presented.

1. Introduction

The structure of nucleon, in the view of recent theoretical developments, is more comprehensively described by the generalized parton distribution (GPDs) functions [1–3]. The GPDs that are off-diagonal extensions of ordinary parton distributions provide a multidimensional description of the nucleon structure in terms of quark and gluon degrees of freedom. In contrast to form factors and parton distribution functions, which are one dimensional distributions, the GPDs contain a correlated information on transverse spatial and longitudinal momentum distributions of partons [4, 5], moreover the elastic form factors and parton distributions appear as moments and limiting cases of GPDs, respectively. Another interesting feature of GPDs is their sensitivity to the total angular momentum of partons in the nucleon according to Ji relation [3].

Experimentally, the GPDs can be accessed through measurements of hard exclusive lepton-nucleon scattering processes. The hard exclusive processes on spin-1/2 nucleon are described by four leading-twist GPDs (H , E , \tilde{H} , and \tilde{E}), while certain experimental observables require a consideration of higher-twist contributions as well. The most commonly used experimental probe of GPDs is the Deeply Virtual Compton Scattering (DVCS) or hard leptonproduction of real photons $\ell + N \rightarrow \ell + N' + \gamma$. During last decade DVCS process was extensively studied from both theoretical and experimental sides. Currently there exist several measurements by HERMES, CLAS, H1, ZEUS and Hall-A experiments. The main observables are the cross-sections, cross-section differences and azimuthal asymmetries. Apart from DVCS a complementary information on GPDs can be obtained from measurements of hard exclusive meson production processes $\ell + N \rightarrow \ell + N' + V$. Unlike DVCS, which is well studied also from the theory side and even effects of next-to-leading order and next-to-leading twist are under control, the situation with hard meson production is in a less advanced stage. First of all the factorisation is proven

^ae-mail: emailaram.movsisyan@desy.de

not for all the amplitudes, thus the interpretation of the observations in terms of GPDs requires more sophisticated measurements with possible separation of different amplitudes. In addition also a good knowledge of meson distribution amplitudes is important. On the other side, measurements of exclusive meson production processes with different final state mesons (ρ , ϕ , ω etc.) provide a unique opportunity to study the GPDs of various flavours.

In a single photon exchange approximation the theoretical description of the hard exclusive meson production processes can be given in two alternative approaches. Throughout many years the features of the process were successfully described in terms of Vector Meson Dominance model [6]. Here the virtual photon, emitted by an incoming lepton, fluctuates into a vector meson, and the interaction of the later one with the nucleon is described using Regge phenomenology. The second approach is based on perturbative QCD description of the process, in terms of handbag diagrams [7]. Here the GPDs are involved in the parameterisation of the non-perturbative part of the diagrams. In pQCD approach the virtual photon dissociates into a $q\bar{q}$ pair, whose interaction with the nucleon results in a formation of final state meson. The interaction can proceed via two distinct mechanisms: quark-antiquark or two-gluon exchange, therefore providing an information also about gluon GPDs. In the Regge picture the interaction mechanism with two-gluon exchange is similar to the exchange of the pomeron, while the interaction mechanism with quark exchange is similar to the exchange of secondary reggeons, with either natural (ω , ρ , a_2) or unnatural (π , a_1) parity. In context of GPDs, the natural parity exchange processes are described by GPDs H and E , while in the description of unnatural parity exchange processes the GPDs \tilde{H} and \tilde{E} are involved. As a consequence, for the proper description of the experimental observables in terms of GPDs, it is of particular importance to distinguish relative contributions of various production mechanisms in the given kinematic conditions of the particular measurement.

The spin transfer from the virtual photon γ^* to the vector meson is commonly described in terms of Spin Density Matrix Elements (SDMEs) [8], which in turn are related to different helicity amplitudes. The scattering of unpolarized leptons off an unpolarized targets is described by 15 SDMEs, while for the scattering of longitudinally polarized leptons off an unpolarized targets, 8 additional SDMEs are required for the description of the process. The SDMEs can be obtained from decay angular distributions in the vector meson production.

In the following section we present the results of SDMEs measured at HERMES, using HERA lepton beam with the energy of 27.6 GeV. The measurements were done on both Hydrogen and Deuterium targets and the results of SDMEs were extracted for ρ , ϕ and ω mesons in the following kinematic range: $1 \text{ GeV}^2 < Q^2 < 7 \text{ GeV}^2$, $-t < 0.4 \text{ GeV}^2$ and $2 \text{ GeV} < W < 6.3 \text{ GeV}$. The extraction of SDMEs was performed using unbinned maximum likelihood fitting technique to fit the azimuthal distributions of decay products. The details of the exclusive event selection, SDME extraction, and the propagation of systematic uncertainties are presented in [9].

2. HERMES results on the production of ρ , ϕ and ω mesons

Results of 23 SDMEs for exclusive ρ^0 and ϕ meson production are presented in Fig. 1 for both Hydrogen and Deuterium targets corresponding to the entire HERMES kinematic range. The SDMEs are grouped into different classes corresponding to different spin transitions between virtual photon and vector meson. The SDMEs measured with unpolarized (polarized) beam are displayed in the unshaded (shaded) areas. The measured SDMEs of class A, that correspond to the diagonal ($\gamma_L^* \rightarrow V_L$ and $\gamma_T^* \rightarrow V_T$) transitions, and class B, that correspond to the interference of the diagonal transition amplitudes, have significant non-zero values for both ρ^0 and ϕ mesons. There is in average 10 – 20% difference between results for ρ^0 and ϕ meson productions. Significant non-zero values of SDMEs of class C are observed for ρ^0 meson. One of the SDMEs differs from zero by more than ten standard deviations of the total experimental uncertainty. This indicates the presence of a production mechanism

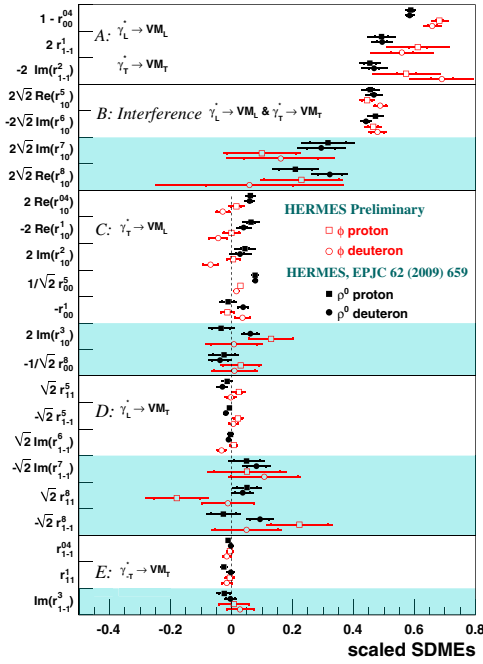


Figure 1. SDMEs of ϕ and ρ^0 mesons.

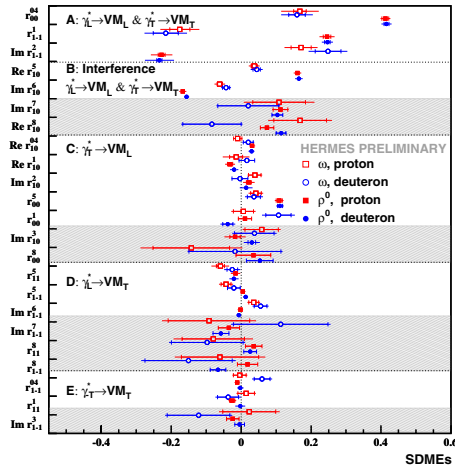


Figure 2. SDMEs of ω and ρ^0 mesons.

that does not conserve s-channel helicity, and the non diagonal transition amplitudes are not negligible for the ρ meson production. The ϕ meson SDMEs of the same class are consistent with zero. The SDMEs of classes D and E are also consistent with zero for both mesons except from the polarized ρ^0 SDMEs, which show slightly positive values. No significant differences are observed between SDMEs measured on Hydrogen and Deuterium targets.

Figure 2 shows the results of 23 SDMEs for exclusive ω meson production on both Hydrogen and Deuterium targets. The results are shown in comparison with the SDMEs for ρ meson. As in the case

of ρ and ϕ mesons, also for the ω meson the SDMEs of classes A and B significantly differ from zero. SDMEs of classes C and E are also consistent with zero, while SDMEs of class D show small deviation from zero, suggesting a violation from s-channel helicity conservation and a presence of non negligible contribution from non diagonal amplitudes. Within the total experimental uncertainty the SDMEs of ω meson measured on both targets are consistent. The comparison between SDMEs for ω and ρ mesons shows significant differences. This can be explained by the significant contribution from the unnatural parity exchange mechanism in the production of ω mesons. Relative contribution of natural and unnatural parity exchange mechanisms can be studied from the measured SDMEs considering the following combinations: $U_1 = 1 - r_{00}^{04} + 2r_{1-1}^{04} - 2r_{11}^1 - 2r_{1-1}^1$, $U_2 = r_{11}^5 + r_{1-1}^5$ and $U_3 = r_{11}^8 + r_{1-1}^8$. Under the assumption that the natural parity exchange mechanism has the dominant contribution, the above given quantities are expected to vanish. Current measurements show that the quantity U_1 for ρ meson has a value of 0.125 and differs from zero by more than two standard deviations of the total experimental uncertainty, suggesting a non negligible contribution from unnatural parity exchange mechanism. The same quantity for the ω meson has also a significant positive value, moreover it is larger than unity, which can be explained by the dominance of unnatural parity exchange amplitudes over the natural parity exchange ones.

From the measured results of SDMEs it is possible to study also the longitudinal-to-transverse cross-section ratio and also phase differences between various amplitudes. These results for the ρ meson production are available in reference [9], and for the ω and ϕ mesons will be available in the upcoming publications.

The presented results of SDMEs and also derived quantities can provide strong constrains on various GPD models and can be used for the fitting various free parameters of the particular GPD model. An example of such a comparison of HERMES results with a specific GPD model is presented in reference [10].

References

- [1] D. Muller, et al., Fortsch. Phys. **42**, 101 (1994)
- [2] A.V. Radyushkin, Phys. Lett. B **380**, 417 (1996); Phys. Rev. D **56**, 5524 (1997)
- [3] X. Ji, Phys. Rev. Lett. **78**, 610 (1997); Phys. Rev. D **55**, 7114 (1997)
- [4] J.P. Ralston, B. Pire, Phys. Rev. D **66**, 111501 (2002)
- [5] M. Burkardt, Phys. Rev. D **62**, 071503 (2000); Erratum-ibid C **31**, 277 (2003)
- [6] J.J. Sakurai, Ann. Phys. **11**, 1 (1960)
- [7] S.J. Brodsky et al., Phys. Rev. D **50**, 3134 (1994)
- [8] K. Schillimng, G. Wolf, Nucl. Phys. B **61** 381 (1973)
- [9] A. Airapetian et al., [HERMES Collab.], EPJ C **62**, 659 (2009)
- [10] S.V. Goloskokov, P. Kroll, EPJ C **53**, 367 (2008)